

Bloch Model Wavefunctions and Pseudopotentials for All Fractional Chern Insulators

Yang-Le Wu,¹ N. Regnault,^{1,2} and B. Andrei Bernevig¹

¹*Department of Physics, Princeton University, Princeton, NJ 08544*

²*Laboratoire Pierre Aigrain, ENS and CNRS, 24 rue Lhomond, 75005 Paris, France*

We introduce a Bloch-like basis in a C -component lowest Landau level fractional quantum Hall effect (FQH), which entangles the real and internal degrees of freedom and preserves an $N_x \times N_y$ full lattice translational symmetry. We implement the Haldane pseudopotential Hamiltonians in this new basis. Their ground states are the model FQH wavefunctions, and our Bloch basis allows for a *mutatis mutandis* transcription of these model wave functions to the fractional Chern insulator of arbitrary Chern number C , obtaining wavefunctions different from Barkeshli and Qi [1]. For $C > 1$, our wavefunctions are related to color-dependent magnetic-flux inserted versions of Halperin and non-Abelian color-singlet states. We then provide large-size numerical results for both the $C = 1$ and $C = 3$ cases. This new approach leads to improved overlaps compared to previous proposals. We also discuss the adiabatic continuation from the FCI to the Bloch-like basis model, both from the energy and entanglement spectrum perspectives.

PACS numbers: 73.43.-f, 71.10.Fd, 03.65.Vf, 03.65.Ud

Recently, several groups showed that gapped topological phases resembling the *fractional* quantum Hall (FQH) effects can be stabilized in a flat band with Chern number $C \neq 0$ by strong electronic interactions in the absence of a magnetic field [2–4]. These are named fractional Chern insulators (FCI). Most of the research efforts have been focused on the case of $C = 1$: in various lattice models [5–8], several groups have provided compelling evidence [2–4, 9–23] for the presence of the Read-Rezayi series [10–12, 24, 25] as well as the composite-fermion [26–28] FQH states. The correlated phases in Chern bands with $C > 1$ [1, 29–32], however, are more intricate. Numerical studies found both bosonic [32–34] and fermionic [33, 35] topological phases resembling the color-SU(C) version of the Halperin [36] and the non-Abelian spin-singlet [37] (NASS) states [34], *but with clear deviations* [34].

To understand these novel topological phases, a series of approaches were put forward. For $C = 1$, one can identify the nature of these states 1) through a folding principle [4, 10] that links the FCI and FQH quantum numbers, 2) through the entanglement spectrum [38, 39] of the ground states [4, 11], and 3) through overlaps with model states obtained from replacing the LLL orbitals with hybrid Wannier states, but leaving the occupation-number weights unchanged [1, 40]. After proper gauge fixing [41], high overlaps were obtained [41–43] from the last approach and FCI-FQH adiabatic continuity was demonstrated [42, 43].

For $C > 1$, the finite-size numerical results are harder to understand. The FCI equivalent of the Halperin states was proposed to occur at Abelian filling factors [1]. The particle entanglement spectrum [34], however, shows clear discrepancy from such states. We are also unable to consistently implement the exclusion principle for colorful FQH model states [44, 45] in the Wannier basis. Naively, a C -component quantum Hall system con-

tains C *decoupled* copies of LLL, each having a unity Chern number over a Brillouin zone (BZ) consisting of $N_\phi = N_x N_y / C$ momenta [10]. This *appears* to be very different from the single Chern number C manifold of the lattice BZ of $N_x N_y$ momenta, especially when $N_x N_y / C \notin \mathbb{Z}$.

In this Letter, we break away from previous approaches and construct in a C -component LLL a *momentum-space* basis that mimics the $N_x \times N_y$ Bloch states in the Chern band. These new one-body basis states entangle the color and the real spaces, and form a single $N_x \times N_y$ Brillouin zone with *flat* Berry curvature and Chern number C , *regardless of* lattice size commensuration with C . This leads to a new mapping between FCI with *arbitrary* C on a lattice of *arbitrary* size and a C -component FQH system. Our mapping operates directly in *Bloch momentum* space and utilizes the *full* lattice translational symmetry, which removes the huge computational cost of [41, 42]. For $C = 1$, our construction is equivalent to the Wannier construction [40], except for a new gauge fixing that improves the overlaps (than [41, 43]). For $C > 1$, our model FCI states are equivalent to a new, color-dependent magnetic-flux inserted version of the Halperin or the NASS states, different from the existing proposal [1]. The FCI wavefunctions produced by our approach have the correct entanglement spectrum [11, 34]. We demonstrate large overlaps for previously unattained sizes between our model FCI wavefunctions and numerics for both $C = 1$ and the uncharted case of $C > 1$.

Consider a translationally-invariant two-dimensional (2D) band insulator on an $N_x \times N_y$ lattice with N_o orbitals per unit cell indexed by b . The Bravais lattice is $m_x \mathbf{b}_x + m_y \mathbf{b}_y$, with $(m_x, m_y) \in \mathbb{Z}^2$ and the primitive translation vectors \mathbf{b}_x and \mathbf{b}_y . We focus on a single Chern band of Bloch states $|\mathbf{k}\rangle$, labeled by momentum $\mathbf{k} = \sum_\alpha k_\alpha \mathbf{g}_\alpha$, with $k_\alpha \in \mathbb{Z}$ and $\mathbf{g}_\alpha \cdot \mathbf{b}_\beta = 2\pi\delta_{\alpha\beta}/N_\beta$

$(\alpha, \beta \in \{x, y\})$. We use $|\mathbf{k}\rangle$ and $|k_x, k_y\rangle$ interchangeably. The orbital b is embedded at ϵ_b relative to its unit cell coordinate in real space [41]. The projected density in the Chern band is [9, 10, 13]

$$\rho_{\mathbf{q}} = \sum_{\mathbf{k}} \left[\sum_b e^{-i\mathbf{q} \cdot \epsilon_b} u_b^*(\mathbf{k}) u_b(\mathbf{k} + \mathbf{q}) \right] |\mathbf{k}\rangle \langle \mathbf{k} + \mathbf{q}|, \quad (1)$$

where $u_b(\mathbf{k})$ is the periodic part of the Bloch wavefunction. At $\mathbf{q} = \mathbf{g}_\alpha$, the bracketed factor in Eq. (1) gives the band geometry through the non-unitary exponentiated Abelian Berry connection, $\mathcal{A}_\alpha = \sum_b e^{-i\mathbf{q} \cdot \epsilon_b} u_b^*(\mathbf{k}) u_b(\mathbf{k} + \mathbf{g}_\alpha)$. $|\mathcal{A}_\alpha(\mathbf{k})|$ contains the quantum distance between $|\mathbf{k}\rangle$ and $|\mathbf{k} + \mathbf{g}_\alpha\rangle$, while $A_\alpha(\mathbf{k}) = \mathcal{A}_\alpha(\mathbf{k})/|\mathcal{A}_\alpha(\mathbf{k})|$ is the unitary Berry connection between them.

The gauge-invariant Wilson loops (geometric phases) can be obtained by parallel transporting around a close loop over the BZ torus. All the contractible loops consist of a product of loops around a single plaquette, namely $\rho_x \rho_y [\rho_y \rho_x]^{-1} = \sum_{\mathbf{k}}^{\text{BZ}} D(\mathbf{k}) W_{\blacksquare}(\mathbf{k}) |\mathbf{k}\rangle \langle \mathbf{k}|$. Here, $D(\mathbf{k}) = |\mathcal{A}_x(\mathbf{k}) \mathcal{A}_y(\mathbf{k} + \mathbf{g}_x) \mathcal{A}_x^{-1}(\mathbf{k} + \mathbf{g}_y) \mathcal{A}_y^{-1}(\mathbf{k})| \in \mathbb{R}$ is related to the non-uniformity of the quantum distance, and $W_{\blacksquare}(\mathbf{k}) = A_x(\mathbf{k}) A_y(\mathbf{k} + \mathbf{g}_x) [A_y(\mathbf{k}) A_x(\mathbf{k} + \mathbf{g}_y)]^\dagger \in \text{U}(1)$ is the unitary Wilson loop around the plaquette with lower-left corner at \mathbf{k} . For large enough N_x and N_y , we can unambiguously extract Berry curvature $f_{\mathbf{k}} = \frac{1}{2\pi} \Im \log W_{\blacksquare}(\mathbf{k})$, with finite-size normalization convention $\sum_{\mathbf{k}}^{\text{BZ}} f_{\mathbf{k}} = C$. \Im takes the imaginary part in the principal branch $\Im \log(z) \in (-\pi, \pi]$. This gives a sharp finite-size formula for the Chern number, $C = \frac{1}{2\pi} \text{Tr} \Im \log [\rho_x \rho_y (\rho_y \rho_x)^{-1}]$. In addition to $W_{\blacksquare}(\mathbf{k})$, there are also two *independent non-contractible* Wilson loops on the torus, related to charge polarizations: the Wilson loop around $k_y = 0$, $W_x = \text{Phase} [\langle \mathbf{0} | \rho_x^{N_x} | \mathbf{0} \rangle] = \langle N_x \mathbf{g}_x | \mathbf{0} \rangle \prod_{\kappa=0}^{N_x-1} A_x(\kappa \mathbf{g}_x)$, with $|\mathbf{0}\rangle \equiv |\mathbf{k} = \mathbf{0}\rangle$, and the Wilson loop W_y around $k_x = 0$ defined similarly.

The structure of geometric phases in the Chern band is fully specified by the collection of the Wilson loops $W_{\blacksquare}(\mathbf{k})$ and W_α , $\alpha = x, y$. We now build a LLL basis in (k_x, k_y) Bloch space, from which all properties of a Chern band with arbitrary Chern number can be translated *mutatis mutandis*. Diagonalizing the Haldane pseudopotentials in this basis gives us the FCI model wavefunctions.

We consider electrons on a (continuum) torus $(\mathbf{L}_x, \mathbf{L}_y) \sim (N_x \mathbf{b}_x, N_y \mathbf{b}_y)$ with twist angle θ in a magnetic field $\mathbf{B} = B \hat{e}_z$. The magnetic translations are $T(\mathbf{d}) = e^{-i\mathbf{d} \cdot \mathbf{K}}$, where $\mathbf{K} = -i\hbar \nabla - e\mathbf{A} + e\mathbf{B} \times \mathbf{r}$. We adopt the Landau gauge $\mathbf{A}(\mathbf{r}) = Bx \hat{e}_y$. The guiding-center periodic boundary conditions $T(\mathbf{L}_\alpha) = 1$ quantize the number of flux quanta $N_\phi = L_x L_y \sin \theta / (2\pi l_B^2)$ to an integer [46]. We set it to $N_\phi = N_x N_y$ in accordance with the Chern insulator [10, 40] for $C = 1$. The usual basis

$\{|j\rangle\}$ in the LLL is

$$\langle x, y | j \rangle = \frac{1}{(\sqrt{\pi} L_y l_B)^{1/2}} \sum_n^{\mathbb{Z}} \exp \left[2\pi(j + nN_\phi) \frac{x + iy}{L_y} - i \frac{\pi L_x e^{-i\theta}}{N_\phi L_y} (j + nN_\phi)^2 \right] e^{-x^2/(2l_B^2)}. \quad (2)$$

To make contact with the Bloch states, we introduce a new LLL basis that diagonalizes translations in both directions, $T(\mathbf{L}_\alpha/N_\alpha) |\mathbf{k}\rangle = e^{-i2\pi k_\alpha/N_\alpha} |\mathbf{k}\rangle$,

$$|\mathbf{k}\rangle = \frac{1}{\sqrt{N_x}} \sum_{m=0}^{N_x-1} e^{i2\pi m k_x/N_x} |j = mN_y + k_y\rangle, \quad (3)$$

where $\mathbf{k} = \sum_\alpha k_\alpha \mathbf{g}_\alpha$ lives on the lattice reciprocal to $(\mathbf{L}_x, \mathbf{L}_y)$. These states are periodic in k_x , $|k_x + N_x, k_y\rangle = |k_x, k_y\rangle$, but *quasi*-periodic [49] in k_y , $|k_x, k_y + N_y\rangle = e^{-i2\pi k_x/N_x} |k_x, k_y\rangle$. Each $|\mathbf{k}\rangle$ satisfies $T(\mathbf{L}_\alpha) = 1$. We find the LLL-projected density in the $|\mathbf{k}\rangle$ basis,

$$\rho_{\mathbf{q}} = e^{-\mathbf{q}^2 l_B^2/4} \sum_{\mathbf{k}}^{\text{BZ}} e^{-i2\pi \mathbf{q} \cdot (\mathbf{k} + \mathbf{q}/2)/N_\phi} |\mathbf{k}\rangle \langle \mathbf{k} + \mathbf{q}|, \quad (4)$$

with $\mathbf{q} = \sum_\alpha q_\alpha \mathbf{g}_\alpha$, $q_\alpha \in \mathbb{Z}$. The Wilson loops are $W_{\blacksquare}(\mathbf{k}) = e^{i2\pi/N_\phi}$, $W_x = e^{-i2\pi k_y/N_y}$, and $W_y = e^{i2\pi k_x/N_x}$.

Using Eq. (4), one can diagonalize any FQH Hamiltonian $\sum_{\mathbf{q}} V_{\mathbf{q}} \rho_{\mathbf{q}} \rho_{-\mathbf{q}}$ (including pseudopotential and even higher-body Hamiltonians), directly in the $|\mathbf{k}\rangle$ basis, and then translate the resulting wavefunction to the FCI by replacing $|\mathbf{k}\rangle$ with the lattice Bloch states. The advantage of the new LLL basis [Eq. (3)] is many-fold. The conditions for the relevance of the FQH state to FCI are explicit in this basis [Eq. (4)]: the Berry curvature must not fluctuate wildly [9] and the quantum distance [50] over the Chern band must fall off with \mathbf{q} rapidly, similar to $e^{-\mathbf{q}^2 l_B^2/4}$. Eq. (4) also allows a much simpler and more effective treatment of the curvature fluctuations in gauge fixing (see below). The most practical advantage of working directly in Bloch basis is the avoidance of the *many-body* Fourier transform in the Wannier prescription. This greatly simplifies the numerical implementation and nearly *squares* the largest Hilbert space dimension that we can study in numerics.

We now turn to the case of $C > 1$ and construct a Bloch-like basis in the C -component LLL with $N_\phi = N_x N_y / C$ fluxes that forms an $N_x \times N_y$ BZ with flat curvature and Chern number C . The starting point is to look for two commuting translation operators that resolve an $N_x \times N_y$ BZ. The finite magnetic translations $T_\alpha = T(\mathbf{L}_\alpha/N_\alpha)$ seem natural, but they do not commute, $T_x T_y = T_y T_x e^{i2\pi/C}$. The cure must come from the color structure of the multi-component system. We assume a *color-neutral* Hamiltonian H . Two color operators P, Q (diagonal in real space) commute with the Hamiltonian,

$$P|\sigma\rangle = |\sigma + 1 \pmod{C}\rangle, \quad Q|\sigma\rangle = e^{i2\pi\sigma/C} |\sigma\rangle. \quad (5)$$

$|\sigma\rangle$, with $\sigma \in \mathbb{Z}_C$, are color eigenstates. Their commutation relation $PQ = QPe^{-i2\pi/C}$ is *complementary* to that of T_x, T_y . The two color-entangled operators $\tilde{T}_x = T_x P$ and $\tilde{T}_y = T_y Q$ commute with each other and H [51]. We define the eigenstates $|\mathbf{k}\rangle$ with $\tilde{T}_\alpha |\mathbf{k}\rangle = e^{-i2\pi k_\alpha/N_\alpha} |\mathbf{k}\rangle$,

$$\langle x, y, \sigma | \mathbf{k} \rangle = \frac{1}{(\sqrt{\pi} N_x L_y l_B)^{1/2}} \sum_n e^{i2\pi(nC+\sigma)k_x/N_x} \exp \left[2\pi \left(k_y + nN_y + \frac{\sigma}{C} N_y \right) \frac{x + iy}{L_y} - i \frac{\pi L_x e^{-i\theta}}{N_\phi L_y} \left(k_y + nN_y + \frac{\sigma}{C} N_y \right)^2 \right] e^{-x^2/(2l_B^2)}. \quad (6)$$

Due to $[T(\mathbf{L}_\alpha), \tilde{T}_\beta] \neq 0$, generically we have to abandon the boundary condition $T(\mathbf{L}_\alpha) = 1$, and adopt the *color-entangled* generalization $\tilde{T}_\alpha^{N_\alpha} = 1$, i.e.

$$T(\mathbf{L}_x) P^{N_x} = T(\mathbf{L}_y) Q^{N_y} = 1. \quad (7)$$

This quantizes k_α to integers. Since $\tilde{T}_\alpha^{N_\alpha}$ commute with each other *by construction*, N_ϕ is *not* restricted to an integer any more, unlike [1]. We *only* require $N_x, N_y, C \in \mathbb{Z}$. The $|\mathbf{k}\rangle$ states are periodic in k_x , but *quasi*-periodic in k_y , $|k_x, k_y + N_y\rangle = e^{-i2\pi k_x C/N_x} |k_x, k_y\rangle$. There are $N_x \times N_y$ independent $|k_x, k_y\rangle$ states, which form a BZ of the *same* size as the lattice and with the *same* Chern number C . After summing over colors, the LLL-projected density operator $\rho_{\mathbf{q}} = \sum_\sigma \rho_{\mathbf{q}\sigma}$ in the *color-entangled* basis $|\mathbf{k}\rangle$ takes *identical* form as in Eq. 4, *except for the generalization* $N_\phi = N_x N_y / C$. The color-entangled BZ has flat curvature $f_{\mathbf{k}} = 1/N_\phi$, as inferred from $W_{\mathbf{k}}(\mathbf{k}) = e^{i2\pi/N_\phi}$. The matrix elements of $\rho_{\mathbf{q}}$ in the C -component LLL, which are the building blocks of the interacting Hamiltonian, are *exactly equal to the C -th power* of those in the single component LLL. Model wavefunctions of pseudopotential Hamiltonians in the $|\mathbf{k}\rangle$ basis can immediately be translated to the FCI with arbitrary C . Further, we can generalize the color-entangled boundary conditions in the LLL to $\tilde{T}_\alpha^{N_\alpha} = e^{-i2\pi\gamma_\alpha}$, where the twist angle $\gamma_\alpha \in \mathbb{R}$ corresponds to flux insertions. This shifts the momentum $\mathbf{k} \rightarrow \mathbf{k} + \boldsymbol{\gamma}$ with $\boldsymbol{\gamma} = \sum_\alpha \gamma_\alpha \mathbf{g}_\alpha$. The connections become $A_\alpha(\mathbf{k} + \boldsymbol{\gamma})$, while the large Wilson loops around $k_\alpha = 0$ are $W_x(\gamma_y) = e^{-i2\pi C \gamma_y / N_y}$ and $W_y(\gamma_x) = e^{i2\pi C \gamma_x / N_x}$.

Linking together the LLL $|\mathbf{k}\rangle$ and the lattice $|\mathbf{k}\rangle$ bases requires one additional step of gauge fixing. The connections over the LLL BZ are $A_x^L(\mathbf{k}) = e^{-i2\pi k_y / N_\phi}$, and $A_y^L(\mathbf{k}) = 1$ (superscript ‘L’ represents LLL). They satisfy the discrete analog of the Coulomb gauge condition [52], i.e. they can be expressed as $A_\alpha^L(\mathbf{k}) = \exp(-i2\pi \sum_\beta \varepsilon_{\alpha\beta} [d_\beta \phi^L]_{\mathbf{k}})$ in terms of a “stream function”, in this case $\phi_{\mathbf{k}}^L = (k_y + 1/2)^2 / (2N_\phi)$. Here, d_β is the backward finite difference operator, defined by $[d_\beta F]_{\mathbf{k}} = F_{\mathbf{k}} - F_{\mathbf{k}-\mathbf{g}_\beta}$, and $\phi_{\mathbf{k}}^L$ satisfies the discrete Poisson equation

with curvature as source, $[\tilde{\Delta} \phi^L]_{\mathbf{k}} = 1/N_\phi$, with discrete Laplacian given by $[\tilde{\Delta} F]_{\mathbf{k}} = \sum_{\mathbf{p}}^{\pm \mathbf{g}_x, \pm \mathbf{g}_y} (F_{\mathbf{k}+\mathbf{p}} - F_{\mathbf{k}})$. We impose the same Coulomb gauge condition on the lattice connections, and handle separately the average and the fluctuations of the lattice BZ curvature:

$$A_\alpha^{\text{target}}(\mathbf{k}) = A_\alpha^L(\mathbf{k} + \boldsymbol{\gamma}) \exp(-i2\pi \varepsilon_{\alpha\beta} [d_\beta \phi]_{\mathbf{k}}). \quad (8)$$

The curvature average necessitates the first factor above. The shift $\boldsymbol{\gamma} = \sum_\alpha \gamma_\alpha \mathbf{g}_\alpha$ with $\gamma_\alpha \in \mathbb{R}$ is determined by $W_x^{\text{lat}} = W_x^L(\gamma_y)$ and $W_y^{\text{lat}} = W_y^L(\gamma_x)$, and it accounts for the mismatch in the large Wilson loops between the two systems. The curvature fluctuations are attended by the exponential factor, where the stream function $\phi_{\mathbf{k}}$ satisfies the discrete Poisson equation $[\tilde{\Delta} \phi]_{\mathbf{k}} = f_{\mathbf{k}} - 1/N_\phi$, with boundary conditions $[d_\alpha \phi]_{\mathbf{k}} = [d_\alpha \phi]_{\mathbf{k}-N_\beta \mathbf{g}_\beta}$ (no summation implied) and $\sum_{\kappa}^{N_x} [d_y \phi]_{\kappa \mathbf{g}_x} = \sum_{\kappa}^{N_y} [d_x \phi]_{\kappa \mathbf{g}_y} = 0$. In plain words, we require that the connection corrections accounting for the curvature fluctuations should be periodic over the lattice BZ [53], and they should not contribute to the large Wilson loops W_α^{lat} which have already been fixed by the $A_\alpha^L(\mathbf{k} + \boldsymbol{\gamma})$ factor. Up to an inconsequential \mathbf{k} -independent constant, these conditions allow a *unique* solution $\phi_{\mathbf{k}} = \varphi_{\mathbf{k}} + v_y k_x - v_x k_y$, with $v_\alpha = \frac{1}{N_\alpha} \sum_{\kappa=0}^{N_\alpha-1} \sum_\beta \varepsilon_{\alpha\beta} [d_\beta \varphi]_{\kappa \mathbf{g}_\alpha}$, and

$$\varphi_{\mathbf{k}} = \frac{1}{N_x N_y} \sum_{\mathbf{n} \neq 0} \frac{e^{i2\pi(k_x n_x / N_x + k_y n_y / N_y)}}{2 \cos(2\pi n_x / N_x) + 2 \cos(2\pi n_y / N_y) - 4} \sum_{\mathbf{p}}^{\text{BZ}} e^{-i2\pi(p_x n_x / N_x + p_y n_y / N_y)} \left(\mathbf{f}_{\mathbf{p}} - \frac{1}{N_\phi} \right), \quad (9)$$

where $\mathbf{n} \equiv (n_x, n_y)$ runs over $\{[0 \dots N_x] \times [0 \dots N_y]\} \setminus (0, 0)$. $A_\alpha^{\text{target}}(\mathbf{k})$ in Eq. (8) is consistent with the actual (fluctuating) curvature over the lattice BZ. Starting from a set of single-particle Bloch states $|\mathbf{k}\rangle$ with an arbitrarily chosen gauge and connections $A_\alpha(\mathbf{k})$, the gauge transform $|\mathbf{k}\rangle \rightarrow e^{i\zeta_{\mathbf{k}}} |\mathbf{k}\rangle$ reproduces $A_\alpha^{\text{target}}(\mathbf{k})$ at $e^{i\zeta_{\mathbf{k}}} = [\prod_{\kappa=0}^{k_y-1} R_y(0, \kappa)] [\prod_{\kappa=0}^{k_x-1} R_x(\kappa, k_y)]$, with $R_\alpha(\mathbf{k}) = A_\alpha^{\text{target}}(\mathbf{k}) / A_\alpha(\mathbf{k})$ [54]. *Any* many-body state $|\Psi\rangle_L$ over the our colorful LLL can be transcribed to the FCI,

$$|\Psi\rangle = \sum_{\{\mathbf{k}\}} e^{i \sum_{\mathbf{k}} \zeta_{\mathbf{k}}} |\{\mathbf{k}\}\rangle \times \mathcal{Z}_L[\{\mathbf{k}\}] |\Psi\rangle_L, \quad (10)$$

where $\mathcal{Z}_L[\{\mathbf{k}\}]$ is the color-entangled occupation-number basis in the LLL with twist $\boldsymbol{\gamma}$ [55].

For FCI with $C > 1$, previous studies suggested that the equivalent FQH states are the $\text{SU}(C)$ color-*singlet* Halperin states [1, 33, 34, 47]. They are the exact zero modes of the *color-neutral* LLL-projected Hamiltonian $H_{\text{FQH}} = \sum_{\mathbf{q}} V_{\mathbf{q}} \rho_{\mathbf{q}} \rho_{-\mathbf{q}}$, where \mathbf{q} is summed over the infinite lattice reciprocal to $(\mathbf{L}_x, \mathbf{L}_y)$ and the interaction between color-neutral densities $\rho_{\mathbf{q}} = \sum_\sigma \rho_{\mathbf{q}\sigma}$ is $V_{\mathbf{q}} = V_0$ for bosons and $V_{\mathbf{q}} = V_0 + (1 - \mathbf{q}^2 l_B^2) V_1$ for fermions, with pseudopotential $V_n > 0$ [56]. For the FQH effect in 2D

electron gas, the boundary conditions $T(\mathbf{L}_\alpha) = 1$ are imposed separately on different color components. In the LLL description of a FCI, however, we require the system to be periodic under the *color-entangled* translations $\tilde{T}_\alpha^{N_\alpha}$. This breaks the $SU(C)$ symmetry. To compare with the Halperin $SU(C)$ -singlet states, we examine the commensurate case $N_x/C \in \mathbb{Z}$. The boundary conditions in Eq. (7) thread $\Phi_\sigma = \sigma N_y/C$ (*color-dependent*) magnetic fluxes along the y direction into the σ -component of the LLL [57]. In the one-dimensional localized basis for LLL [Eq. (2)], this shifts the Landau orbitals of color σ by $\Phi_\sigma \mathbf{L}_x/N_\phi$ in real space. Hence we propose that the Wannier mapping [1] be modified to identify the hybrid Wannier states with our shifted LLL orbitals. In the generic, non-commensurate case, translation $T(\mathbf{L}_x)$ *changes the color* of the particle, due to $T(\mathbf{L}_x)P^{N_x} = 1$. Our construction thus provides a finite-size realization of the “worm-hole” connecting different color components [1].

We demonstrate the Bloch construction using the ruby lattice model ($C = 1$) [8] and the two-orbital triangular lattice model ($C = 3$) [31]. We construct the FCI model states through Eq. (10) from the exact-diagonalization ground states of H_{FQH} with *color-entangled* boundaries. We find high overlaps (Fig. 1a) and identical low-energy structure in the entanglement spectrum with the FCI ground states [11, 34]. The 12-fermion Laughlin state on the ruby lattice model has a Hilbert space of dimension 3.4×10^7 . This state is well captured by the model wave function obtained from our construction (overlap ≈ 0.99). The triangular lattice model has decent overlaps, albeit lower than the ruby lattice model.

To further examine our construction for $C > 1$, we study the interpolation Hamiltonian $H_\lambda = (1 - \lambda)H_{\text{FCI}} + \lambda H_{\text{FQH}}$, $0 \leq \lambda \leq 1$ [42, 43]. For bosonic on-site density-density interaction on the triangular lattice, $H_{\text{FCI}} = U \sum_{ab} \sum_{\{\mathbf{k}_{1-3}\}} \tilde{\psi}_{\mathbf{k}_1 a}^\dagger \tilde{\psi}_{\mathbf{k}_2 b}^\dagger \tilde{\psi}_{\mathbf{k}_3 b} \tilde{\psi}_{\mathbf{k}_4 a}$, where $\mathbf{k}_4 = \mathbf{k}_1 + \mathbf{k}_2 - \mathbf{k}_3 \pmod{N_\alpha \mathbf{g}_\alpha}$, and $\tilde{\psi}_{\mathbf{k}b}^\dagger = e^{i\zeta_{\mathbf{k}}} u_b^*(\mathbf{k}) \psi_{\mathbf{k}}^\dagger$ is gauge-fixed by $e^{i\zeta_{\mathbf{k}}}$, with $|\mathbf{k}\rangle = \psi_{\mathbf{k}}^\dagger |\emptyset\rangle$. For H_{FQH} , we use color-entanglement boundary conditions γ . We find that the FCI model states are adiabatically connected to the actual ground states: H_λ remains gapped for $\lambda \in [0, 1]$ and its ground states retain the characters of the FCI model states as seen in both overlaps and particle entanglement spectrum (Fig. 1b-d). As observed in [34], the 6-boson state on 6×4 lattice has clear deviations from the usual Halperin state in the entanglement spectrum. Our FCI model state exactly reproduces these novel features. Note that the 8×4 lattice is closer to the thin-torus limit [48], resulting in smaller overlaps and $\Delta\xi$ values.

In this Letter, we introduce a Bloch basis for multicomponent LLL with *rational* number of fluxes that entangles real and internal spaces on the *one-body* level. We establish a Bloch-basis mapping between a Chern band with an *arbitrary* Chern number C on an *arbitrary* $N_x \times N_y$ lattice

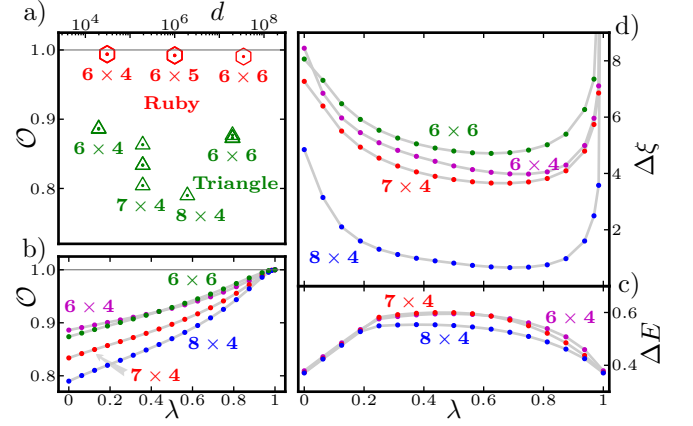


FIG. 1: Panel a) shows the overlaps \mathcal{O} between our FCI model states and the ground states of the fermionic ruby and the bosonic triangular lattice models, as a function of the Hilbert space dimension d . Panels b-d) demonstrate the adiabatic continuity between the triangular lattice model and the color-entangled Halperin pseudopotential Hamiltonian on 6×4 , 7×4 , 8×4 , and 6×6 lattices ($\nu = 1/4$ filling). We set $U = 7.4237, 7.0003, 6.9677$, and 5.0955 resp. to equalize the energy gaps at $\lambda = 0, 1$. Panel b) shows the overlaps \mathcal{O} between our FCI model states and the ground states of the interpolation Hamiltonian H_λ . Panel c) shows the energy gap ΔE above the ground states of H_λ . Panel d) shows the entanglement gap $\Delta\xi$ of the ground states of H_λ . $\Delta\xi$ is defined as the gap between the low-lying structure identical to the full entanglement spectrum of the model states (at $\lambda = 1$) and the higher levels. By this definition, $\Delta\xi$ is infinity at $\lambda = 1$.

and a C -component LLL with $N_\phi = N_x N_y / C \in \mathbb{Q}$ fluxes. This mapping leads to a novel scheme, which we call Bloch construction, to build FCI model states from *color-neutral* FQH Hamiltonians. It treats bosonic/fermionic FCI with arbitrary $N_x, N_y, C \in \mathbb{Z}$ in a *wholesale* fashion, and can handle large system sizes. The new gauge fixing in our basis significantly improves the overlaps with the actual ground states when curvature strongly fluctuates.

We refer to the constructed FCI model states as the *color-entangled* Halperin states. They are distinct from the $SU(C)$ -singlet Halperin states due to the *color-entangled* boundary conditions. When the lattice size is commensurate with C , the *color-entangled* states are the generalization of the usual Halperin states to *color-dependent* twisted boundaries. More generally, the lattice setup opens up access to the *color-entangled, unphysical* sectors of a multicomponent FQH system in a *physical* way. Our new formalism can be applied to the NASS states, and can be used to extract the exclusion principle for the counting of low-lying levels in the energy and the entanglement spectra.

We wish to thank F.D.M. Haldane, C. Fang, and B. Estienne for inspiring discussions, and thank A. Sterdyniak and C. Repellin for collaborations on related work. BAB and NR were supported by NSF CAREER DMR-095242, ONR-N00014-11-1-0635, ARMY-

245-6778, MURI-130-6082, Packard Foundation, and Keck grant. YLW was supported by NSF CAREER DMR-095242.

-
- [1] M. Barkeshli and X.-L. Qi, Physical Review X **2**, 031013 (2012).
- [2] D. N. Sheng, Z.-C. Gu, K. Sun, and L. Sheng, Nature Communications **2**, 389 (2011).
- [3] T. Neupert, L. Santos, C. Chamon, and C. Mudry, Physical Review Letters **106**, 236804 (2011).
- [4] N. Regnault and B. A. Bernevig, Phys. Rev. X **1**, 021014 (2011).
- [5] F. D. M. Haldane, Physical Review Letters **61**, 2015 (1988).
- [6] K. Sun, Z. Gu, H. Katsura, and S. Das Sarma, Physical Review Letters **106**, 236803 (2011).
- [7] E. Tang, J.-W. Mei, and X.-G. Wen, Physical Review Letters **106**, 236802 (2011).
- [8] X. Hu, M. Kargarian, and G. A. Fiete, Physical Review B **84**, 155116 (2011).
- [9] S. A. Parameswaran, R. Roy, and S. L. Sondhi, Physical Review B **85**, 241308 (2012).
- [10] B. A. Bernevig and N. Regnault, Physical Review B **85**, 075128 (2012).
- [11] Y.-L. Wu, B. A. Bernevig, and N. Regnault, Physical Review B **85**, 075116 (2012).
- [12] Y.-F. Wang, H. Yao, Z.-C. Gu, C.-D. Gong, and D. N. Sheng, Physical Review Letters **108**, 126805 (2012).
- [13] M. O. Goerbig, The European Physical Journal B **85**, 15 (2012).
- [14] R. Roy, ArXiv e-prints (2012), 1208.2055.
- [15] J. W. F. Venderbos, S. Kourtis, J. van den Brink, and M. Daghofer, Physical Review Letters **108**, 126405 (2012).
- [16] Y.-F. Wang, Z.-C. Gu, C.-D. Gong, and D. N. Sheng, Physical Review Letters **107**, 146803 (2011).
- [17] T. Neupert, L. Santos, S. Ryu, C. Chamon, and C. Mudry, Physical Review B **84**, 165107 (2011).
- [18] T. Neupert, L. Santos, C. Chamon, and C. Mudry, ArXiv e-prints (2012), 1207.3747.
- [19] G. Murthy and R. Shankar, ArXiv e-prints (2011), 1108.5501.
- [20] G. Murthy and R. Shankar, ArXiv e-prints (2012), 1207.2133.
- [21] S. Kourtis, J. W. F. Venderbos, and M. Daghofer, ArXiv e-prints (2012), 1208.3481.
- [22] C. H. Lee, R. Thomale, and X. L. Qi, ArXiv e-prints (2012), 1207.5587.
- [23] Y. H. Wu, J. K. Jain, and K. Sun, ArXiv e-prints (2012), 1207.4439.
- [24] G. Moore and N. Read, Nuclear Physics B **360**, 362 (1991).
- [25] N. Read and E. Rezayi, Physical Review B **59**, 8084 (1999).
- [26] J. K. Jain, Phys. Rev. Lett. **63**, 199 (1989).
- [27] T. Liu, C. Repellin, B. A. Bernevig, and N. Regnault, ArXiv e-prints (2012), 1206.2626.
- [28] A. M. Läuchli, Z. Liu, E. J. Bergholtz, and R. Moessner, ArXiv e-prints (2012), 1207.6094.
- [29] F. Wang and Y. Ran, ArXiv e-prints (2011), 1109.3435.
- [30] M. Trescher and E. J. Bergholtz, ArXiv e-prints (2012), 1205.2245.
- [31] S. Yang, Z. C. Gu, K. Sun, and S. Das Sarma, ArXiv e-prints (2012), 1205.5792.
- [32] Y. F. Wang, H. Yao, C. D. Gong, and D. N. Sheng, ArXiv e-prints (2012), 1204.1697.
- [33] Z. Liu, E. J. Bergholtz, H. Fan, and A. M. Laeuchli, ArXiv e-prints (2012), 1206.3759.
- [34] A. Sterdyniak, C. Repellin, B. A. Bernevig, and N. Regnault, ArXiv e-prints (2012), 1207.6385.
- [35] A. G. Grushin, T. Neupert, C. Chamon, and C. Mudry, ArXiv e-prints (2012), 1207.4097.
- [36] B. I. Halperin, Helv. Phys. Acta **56**, 75 (1983).
- [37] E. Ardonne and K. Schoutens, Phys. Rev. Lett. **82**, 5096 (1999).
- [38] H. Li and F. D. M. Haldane, Physical Review Letters **101**, 010504 (2008).
- [39] A. Sterdyniak, N. Regnault, and B. A. Bernevig, Physical Review Letters **106**, 100405 (2011).
- [40] X.-L. Qi, Physical Review Letters **107**, 126803 (2011).
- [41] Y.-L. Wu, N. Regnault, and B. A. Bernevig, Physical Review B **86**, 085129 (2012).
- [42] T. Scaffidi and G. Moller, ArXiv e-prints (2012), 1207.3539.
- [43] Z. Liu and E. J. Bergholtz, ArXiv e-prints (2012), 1209.5310.
- [44] B. Estienne and B. A. Bernevig, Nuclear Physics B **857**, 185 (2012).
- [45] E. Ardonne and N. Regnault, Physical Review B **84**, 205134 (2011).
- [46] F. D. M. Haldane, Phys. Rev. Lett. **55**, 2095 (1985).
- [47] Y. M. Lu and Y. Ran, ArXiv e-prints (2011), 1109.0226.
- [48] B. A. Bernevig and N. Regnault, ArXiv e-prints (2012), 1204.5682.
- [49] The non-periodicity signals an topological obstruction to a periodic smooth gauge (Chern number $C = 1$) in the continuum limit.
- [50] To be precise, *one minus* the quantum distance as usually defined.
- [51] Alternatively, we can also use the operator pair $(T_x Q, T_y P^\dagger)$ to define the momentum eigenstates. This amounts to substituting the color-eigenstate $|\sigma\rangle$ in $|\mathbf{k}\rangle$ to $|t\rangle \equiv \frac{1}{\sqrt{C}} \sum_{\sigma=0}^{C-1} e^{i2\pi t\sigma/C} |\sigma\rangle$, For our purpose of obtaining a FCI model state, this change is just a trivial unitary transform that leaves the color-neutral Hamiltonian intact.
- [52] In the continuum limit [41], the exponentiated connections become $A_\alpha(\mathbf{k}) \approx e^{i\mathbf{a}(\mathbf{k}) \cdot \mathbf{g}_\alpha}$, where $\mathbf{a} = -i\langle u_{\mathbf{k}} | \nabla_{\mathbf{k}} | u_{\mathbf{k}} \rangle$ is the Berry connection, with $|u_{\mathbf{k}}\rangle$ being the periodic part of the Bloch state. The Coulomb gauge condition on $\mathbf{a}(\mathbf{k})$ is $\nabla_{\mathbf{k}} \cdot \mathbf{a}(\mathbf{k}) = 0$. This enables one to write the connection in terms of a stream function $\phi(\mathbf{k})$, $\mathbf{a}(\mathbf{k}) = \hat{e}_z \times \nabla_{\mathbf{k}} \phi(\mathbf{k})$. Since $\nabla_{\mathbf{k}} \times \mathbf{a}(\mathbf{k}) = F(\mathbf{k}) \hat{e}_z$, $\phi(\mathbf{k})$ satisfies a Poisson equation $\nabla_{\mathbf{k}}^2 \phi(\mathbf{k}) = F(\mathbf{k})$, where $F(\mathbf{k})$ is the Berry curvature with the usual normalization $\int d^2\mathbf{k} F(\mathbf{k}) = 2\pi C$.
- [53] The obstruction to simultaneous smoothness and periodicity is manifested in the non-fluctuating part $A_\alpha^L(\mathbf{k} + \gamma)$.
- [54] Despite the formal similarity of $e^{i\zeta_{\mathbf{k}}}$ expressed as a product of ratios of connections, our gauge choice here is fundamentally different from the “parallel-transport” gauge [41] in the treatment of the curvature *fluctuations*, embodied in the carefully constructed $A_\alpha^{\text{lat}}(\mathbf{k})$.

- [55] For actual lattice calculations, it is desirable to use periodic gauge with $|\mathbf{k}\rangle = |\mathbf{k} + N_\alpha \mathbf{g}_\alpha\rangle$ (no sum implied). Simply restricting \mathbf{k} to a single BZ would achieve this, as long as the BZ choice for the lattice system is consistent with that for the LLL.
- [56] We focus only on the color-singlet states as observed in numerics [34].
- [57] We have verified by numerical diagonalization that the eigenstates of H_{FQH} with color-entangled boundary conditions indeed coincide with the usual Halperin states with Φ_σ flux insertion, when $N_x/C \in \mathbb{Z}$.